Nonlinear Dyn (2025) 113:4511–4529
https://doi.org/10.1007/s11071-024-10424-1

RESEARCH

Nonlinear analysis of hydrodynamics of a shallow-draft floating wind turbine

Alicia Terrero-Gonzalez · Saishuai Dai · Jim Papadopoulos · Richard. D. Neilson · Marcin Kapitaniak

Received: 30 April 2024 / Accepted: 25 September 2024 / Published online: 16 October 2024

Abstract This study investigates numerically the dynamic responses of the T-Omega Wind novel concept of Floating Offshore Wind Turbine. The turbine is light-weight, has a shallow-draft and a relatively high centre of gravity that allows it to glide over harsh marine environments. The turbine responses are studied under regular wave excitation, considering most probable ranges of discrete sea wave heights and periods representative of real ocean conditions. A multibody virtual model is developed, simplified to a rigid 6 DOF system and experimentally validated in the state-of-art Marine Simulator to define the types of dynamical responses for both *"Low"* and *"High" Sea States*. The dynamics of coupled heave and pitch DOFs are evaluated with time histories, phase-plane portraits, Poincaré sections and FFT analyses to conclude that period-1 stable solutions exist for all studied cases of *"Low Sea States"*, whereas period-2, period-3 and period-4 periodic responses are identified for short wave periods of excitation under *"High Sea States"* conditions. Simulation results show that regions where period-1 responses exist are highly sensitive to wave height and can widen as the wave amplitude reduces. Finally, the turbines' nonlinearities generated by the floats' geometry are observed in this dynamical system, which are identified to be related to variation in float waterplane area and particularly observable for *"High Sea States"*.

Keywords Floating offshore wind turbine (FOWT) · Nonlinear dynamic responses · Shallow draft · Marine simulator · Regular waves

A. Terrero-Gonzalez· R. D. Neilson · M. Kapitaniak (✉)
National Decommissioning Centre, School of Engineering, University of Aberdeen, Newburgh, UK
e-mail: marcin.kapitaniak@abdn.ac.uk

S. Dai
Department of Naval Architecture, Ocean and Marine Engineering, University of Strathclyde, Glasgow, UK

J. Papadopoulos
T-Omega Wind Inc., Boston, USA

1 Introduction

Floating Offshore Wind Turbines (FOWTs) have experienced rapid development in recent years, aiming to harness energy from steadier and stronger wind resources found in deeper waters (≥ 60 ms), where traditional fixed-bottom wind turbines are not feasible [1]. The largest FOWT farm, named the "Hywind Tampen farm", is situated in Norway with an installed capacity of 88 MW [2], followed by "Kincardine" (47.5 MW) [3] and "Hywind Scotland" (30 MW) [4] projects in the North-East of Scotland. The necessity for technological improvement has spurred an expansion of novel FOWT concepts. However, most of these concepts are typically sized only in the order of a few megawatts of capacity (usually not surpassing 10 MW) [5,6] and pose technical challenges related to their structural stability, experimental testing, installation and maintenance [7]. Hence, the dynamical behaviour of typical FOWTs planned (Spar, Tension Leg Platforms, semi-

submersible and barge) have been widely studied to better understand their performance and behaviour under different sea states (i.e. conventional and extreme wave and wind parameters) [8]. Additionally, optimizing the design configurations to prevent their natural frequencies from coinciding with typical sea wave frequencies has been of particular interest [9–11].

The dynamic responses of a FOWT and dynamic loads acting on a multi-body system have been numerically investigated by Luo et al. [12], using a coupled 14-DOF model of a semi-submersible FOWT comprising of a floating platform, tower, nacelle, blades and mooring. The Equations Of Motion (EOM) are derived with the Lagrangian approach to evaluate system responses under combined wave/wind external loads, and validate the results against numerical simulation by FAST software. Similarly, Bagherian et al. [13] presented a 7-DOF model of a semi-submersible FOWT, that takes into account gyroscopic effects. Their study concluded that the rotor's gyroscopic moment does not significantly influence the platform motion response. The dynamics of a spar type FOWT was evaluated by Al-Solihat and Nahon [14] and by Al-Solihat et al. [15], where the first paper presents a 6-DOF nonlinear multibody system consisting of a rigid platform elastically coupled to a rigid tower, with EOM derived with Lagrange method. That model has been validated against FAST [16], HAWC2 [17] and Bladed [18] codes. Their study showed that greater tower flexibility leads to a higher damping and larger yaw amplitude responses compared to rigid towers. Later, Al-Solihat et al. [15] proposed a 7-DOF model comprising of the floating platform, tower, nacelle, rotor and mooring system under combined wind/wave loads, which showed that platform displacements are insensitive to rotor's gyroscopic effects. In addition, Takata et al. [19] experimentally showed that elastic deformation affects the heave responses of a FOWT for wave periods close to the float's resonant periods. Moreover, large amplitude motions of a Spar type were investigated by Wang and Sweetman [20], where the nonlinear dynamic behaviour of an 8-DOF model that includes nonlinear coupling between the translational and rotational DOFs. Lee et al. [21] studied the dynamics of a combined rigid-flexible-body FOWT using Kane's method, where the modal shapes and system's natural frequencies are evaluated considering linearization around the steady state solution.

To evaluate the nonlinear hydrodynamic loads acting on the FOWT, wave height (H), wave period (T) and water depth (D) are the main parameters to be considered when choosing the most accurate wave theory and computational methodology [22]. Computational Fluid Dynamics (CFD) models evaluate accurately viscous, radiation and diffraction effects, thus Ha et al. [23] numerically studied a 15 MW TLP utilizing CFD and a deforming mesh to investigate the system's nonlinear phenomena under irregular wave excitation (JONSWAP spectrum) for extreme wave conditions. Zhou et al. [24] researched the dynamics of a 5 MW semi-submersible FOWT for regular and focused waves and validated the results with two reduced-order potential flow methods using Électricité de France (EDF) [25] and FAST codes. Furthermore, Wang et al. [26] studied the accuracy of CFD simulations of a semi-submersible FOWT under regular waves and those results were experimentally validated. This study generalized a procedure for simulation verifications. Other methods commonly used to evaluate the dynamics of offshore structures are the Morison equation, potential flow/diffraction theory and the hybrid approach, which have been applied to study FOWT dynamics in [27–29].

Dynamical studies of FOWTs subjected to wind/wave loads will provide higher fidelity results if they are performed with a coupled hydro-aero-elastic models [22]. However, due to the complexity of experimental procedures and limitations of the facilities, some novel FOWT concepts are initially studied with decoupled wave and wind models. These types of investigation neglect the coupling between environmental loads and are particularly utilized to evaluate the influence of a specific design or environmental parameter (i.e. float size, wave frequency and/or height) on the nonlinear dynamic behaviour of a structure. Such a study was presented in Patryniak et al. [30], where the sensitivity of a FOWT Instantaneous Centre of Rotation (ICR) to wave height and frequency was studied under regular and irregular waves. Despite the utility of the decoupled analysis, it might be necessary to perform the coupled analysis with hydro-aero-servo-elastic models to accurately take into account the model's aerodynamics, hydrodynamics and the elastic interactions between the assembly components since neglecting the coupling may result in an over optimistic design. This is of particular interest for novel FOWT concepts [31] and new model validations [32]. To perform this type of

coupled analysis, simulations are computed with CFD methods or state-of-art verified simulation tools, such as FAST [33], Bladed, HAWC2 or the Marine Simulator [34,35], amongst others. This study will utilise the state-of-art real time Marine Simulator available at the National Decommissioning Centre (NDC) to conduct analysis to evaluate the dynamical behaviour of a FOWT concept under regular wave excitation based on a numerical model and validated with scaled experimental wave tank results. This approach lies on the highest fidelity spectrum of models of real-time hybrid simulations (RTHS), which utilizes the Linear Wave Theory for waves with small steepness ($H/\lambda < 0.05$) and 2nd order non-linear waves for greater steepness.

To evaluate the nonlinear dynamics of a FOWT in its time-frequency domain previous studies have been performed under wave excitations including regular waves [36], irregular waves (JONSWAP [37] and Pierson-Moskowitz [38] spectrums) and special cases with different wave profiles [39,40]. This has been done along with the evaluation of RAOs (Response Amplitude Operators) for the 6-DOF (surge, sway, heave, roll, pitch and yaw) and their frequency spectrum study [33] for the identification of eigenfrequencies. Natural frequencies are of high importance in such considerations mainly due to the DOF coupling effects. Therefore, this paper focuses on the coupling between heave and pitch motions, where previous experimental studies showed that for semi-submersible FOWT, this coupling effect is especially noticeable when floats present a non-negligible angular displacement close to heave's natural frequency [41]. In addition, the action of coupled environmental loads, such as wind-wave interaction with turbine's structure, could be beneficial from the point of view of system dynamics. In some cases, wind loads restrict frequency components near the turbine's natural frequencies for surge and pitch eigenfrequencies, as previously reported by Tian et al. [42]. The limitation of pitch natural frequency could improve FOWT motion amplitudes, where the maximum angular displacement threshold for good turbine performance is estimated at 10 [deg] [43]. Moreover, the turbine oscillations periodicity and type of system response vary depending on environmental loads and model parameters. An example is presented by Ghabraei et al. [44], who showed that adding mass to the system and/or including lateral vibration absorbers can shift the turbine's response from periodic to quasi-periodic. Hence, the response type and classification will be considered in this study.

This paper presents the hydrodynamical study of a novel light shallow-draft FOWT concept designed by T-Omega Wind Inc [34,45]. The system has a relatively high Centre of Gravity (COG) and low natural period, permitting it to glide over harsh marine environments with extreme wave parameters and is designed for a full-scale capacity of 10 MW. Its stiff and light structure is stabilized and sustained by four hydrostatically stiff cone-shaped interconnected floats and anchored to the seabed with a Single Mooring Point (SMP) system providing the weathervane effect. Common types of SMP for floating turbines are considered in [46], where several catenary mooring lines are connected to a single point of connection without interfering with the weathervane effect and avoiding a structural collapse in case of a single line failure. The multibody model implemented in the Marine Simulator has been previously calibrated and validated with experimental results performed with a 1:60 scaled prototype in a wave tank at the Kelvin Hydrodynamics Laboratory (KHL) at the University of Strathclyde under regular wave excitations. Further information about the experimental procedures, model validation and analytical approximations of system responses can be found in our previous work [34].

The structure of this paper is as follows. In Sect. 2 the novel FOWT concept is described and its model configuration is presented. In addition, a multibody virtual model reduced to 6 DOF is presented concurrently. The methodology of this study is presented in Sect. 3, where the turbine RAOs for *"Low"* and *"High" Sea States* obtained from simulations and experiments are presented. Next, simulation results to evaluate the heave and pitch dynamics are presented in Sect. 4, where the evolution of periodic-type responses for both DOF is discussed in detail, including effects related to hydrodynamic nonlinearities that have been observed. Finally, Sect. 5 concludes with a summary of the main findings studied in this paper and gives some suggestions for future research paths.

2 System description

The T-Omega Wind concept is a shallow-draft FOWT rigid-flexible multibody dynamical system that comprises four rigid bodies that are elastically coupled.

It is shown in Fig. 1a and consists of a rigid floating structure, comprising a cantilevered "Standoff" support interconnecting four cone-shaped floats, which provide buoyancy to the system; a "four-legged" stiff turbine Tower structure, supported by the floats and constructed from a robust series of hollow pipes contributing to the system's lightweight design; a generator and a 3-bladed turbine rotor mounted on top of the tower. The rigid bodies are elastically coupled with a high stiffness and the whole assembly is anchored to the seabed using a single elastic mooring line, which introduces a weathervane effect. This study simplifies the turbines' SMP system in a single mooring line to set the base for future reliability studies to find the most suitable mooring point system for this specific design. Consequently, each assembly component has the following respective properties,

- *Body 1* Floating structure with mass m_f, elastically coupled to the tower through its equally spaced floats with stiffness k_f.
- *Body 2* "Tower" structure of mass m_t supported by the floating structure and coupled at the nacelle to the turbine rotor of stiffness k_t and turbine generator of stiffness k_g.
- *Body 3* Turbine generator of mass m_g attached to the rotor and tower.
- *Body 4* 3-bladed rigid Horizontal Axis Wind Turbine (HAWT) rotor of mass m_b, where no gyroscopic effect is considered. In other words, the focus is on non-operational conditions.

Each component of the assembly has 6 DOF, resulting in a total of 24 DOF system. These bodies are elastically coupled, with a stiffness denoted as k_i, where i signifies the set of couplings between two consecutive bodies. The previous experimental studies ignored the stiffness between different components assuming a rigid body. Hence, to match the experimental conditions the stiffness was set to infinite even though simulations allow compliant components. This permits the multibody system to be reduced to a rigid-body model with just 6-DOF (surge, sway, heave, roll, pitch and yaw) around its COG. Additionally, the FOWT is subjected to excitation from incident regular waves perpendicular to its axis of gyration, which induces external hydrodynamic loads acting on the rigid bodies. Hence, the system dynamics can be described in matrix form by Eq. 1,

$$[M]\{\ddot{\mathbf{a}}\} + [C]\{\dot{\mathbf{a}}\} + [K]\{\mathbf{a}\} = \{\mathbf{F}\}, \tag{1}$$

where $\mathbf{a}$ contains the 6 DOF vector of time dependent state variables defined as $\{\mathbf{a}\} = [x(t), y(t), z(t), \varphi_x(t), \varphi_y(t), \varphi_z(t)]^T$. The variables $x(t)$, $y(t)$ and $z(t)$ denote surge, sway and heave displacements, while $\varphi_x(t)$, $\varphi_y(t)$ and $\varphi_z(t)$ denote roll, pitch and yaw angular displacements, respectively. M is the matrix containing the mass and inertia of each body, C is the damping coefficients matrix and K contains the stiffness coefficients between the coupled bodies. The external hydrostatic, hydrodynamic and mooring forces, such as buoyancy, drag/lift, radiation, diffraction and incident forces acting on the system are contained in $\mathbf{F(t)}$. Concurrently, the model considers approximations of second-order nonlinear loads by utilizing the Quadratic Transfer Function (QTF) and Newman's approximation. An example of these second order loads is the second order drift force, which is evaluated with Eq. 2 [34]

$$\begin{aligned}\vec{F}^2 = &-\oint_{WL} \frac{1}{2}\,\rho\,\xi_r^{(1)}\cdot\,\xi_r^{(1)}\,\hat{\boldsymbol{n}}\,dL \\ &+\iint_{Sb}\frac{1}{2}\rho\,|\nabla\phi^{(1)}|^2\hat{\boldsymbol{n}}\,dS \\ &+\iint_{Sb}\rho\left(a\cdot\nabla\frac{\partial\phi^{(1)}}{\partial t}\right)\hat{\boldsymbol{n}}\,dS + M_s\,R\cdot\ddot{a} \\ &+\iint_{Sb}\rho\,\frac{\partial\phi^{(2)}}{\partial t}\,\hat{\boldsymbol{n}}\,dS\,,\end{aligned} \tag{2}$$

where ϕ^1 and ϕ^2 are the first- and second-order velocity potential, M_s is the mass of the floating body, R the matrix of rotation and WL denotes waterline limit. ρ is the water density, $\xi_r^{(1)}$ is the wave elevation of the first order and Sb represent the body submerged surface area. $\hat{\boldsymbol{n}}$ represents the unit vector normal to the surface. Even though this research treats the turbines' system as a rigid body, the Marine Simulator divides the object into small cells with a gradual mesh and evaluates the response of each rigid body in the 6 DOF. The forces are calculated for each cell within the mesh (see Fig. 1a for mesh representation) and applied to the objects CoG. Hence, for each section Cummins' equation describes the motion of the floating structure in the time domain. This is a common approach while applying the linear wave theory. Therefore, the equation of motion (Eq. 3) is described as follows,

$$\begin{aligned}&(I + I_\infty)\,\ddot{a}(t) + \int_0^t \tilde{K}(t-\tau)\,\dot{a}(\tau)\,d\tau + E\,a(t) \\ &\quad = F^{ext}(t),\end{aligned} \tag{3}$$

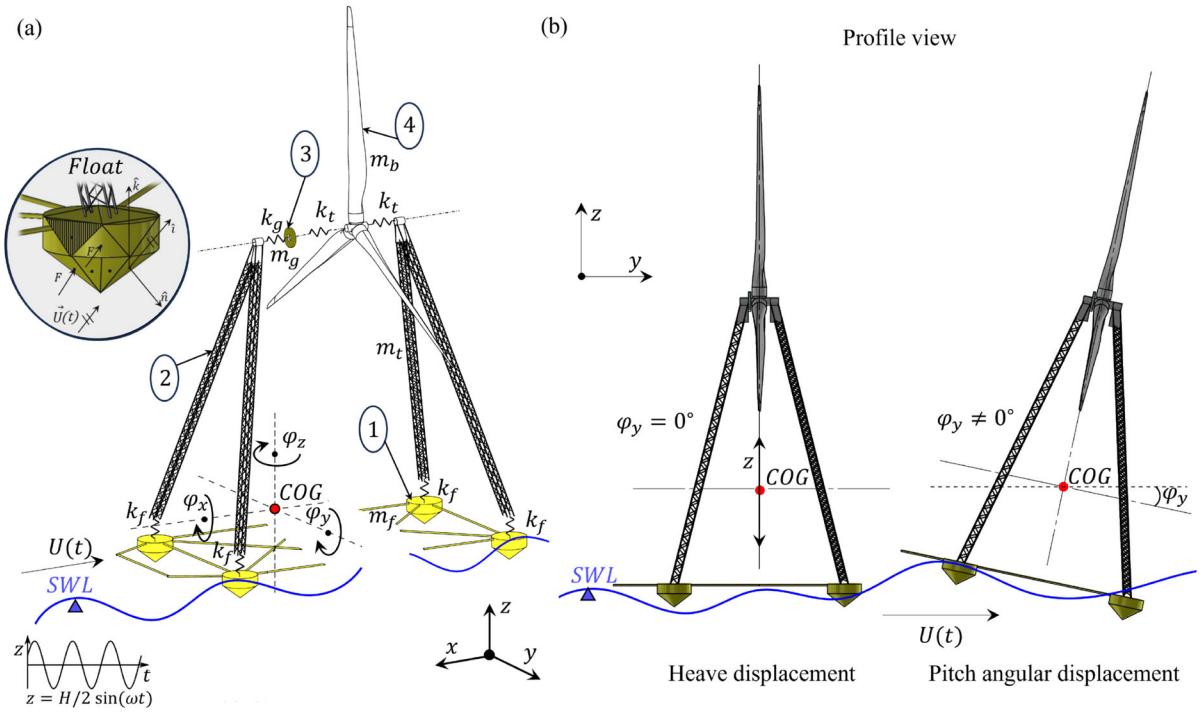

Fig. 1 Multibody dynamical model of T-Omega Wind FOWT under regular wave excitation. **a** Model schematic showing main components of the system (1-Floating structure, 2-"Tower", 3-Generator and 4-Rotor), elastic interactions and hydrodynamic forces acting on the system. Yellow coloured areas are filled with air volumes providing the system with buoyancy. **b** Heave (vertical displacement) and pitch (angular displacement) motions under regular wave excitation perpendicular to turbine axis of gyration in respect to its Centre of Gravity (COG)

in which the radiation force is represented in Eq. 4 as,

$$F_{radiation} = -I_\infty \ddot{a}(t) - \int_0^t \tilde{K}(t-\tau)\,\dot{a}(\tau)\,\delta\tau, \quad (4)$$

where I denotes the structure mass and I_∞ denotes the added mass at an infinity frequency. E is the restoring hydrostatic coefficient, $F^{ext}(t)$ represent all the external acting forces on the turbine and $\tilde{K}(t)$ is the retardation or fluid memory function [47,48]; τ denotes the computation time difference. To solve the Cummins' convolution integral, the simulations utilize inverse Fourier Transformation and its solution is presented in Eq. 5 for every instant computed t as follows,

$$\tilde{K}(t) = \frac{2}{\pi}\int_0^\infty C(\omega)\,cos(\omega t)\,d\omega, \quad (5)$$

where C denotes the damping coefficient for each wave frequency (ω). Finally, all solutions are incorporated in Eq. 1 and the stiffness matrix of coefficients containing the couplings amongst each rigid body are included. Detailed information about the modelling methods can be found in our previous work [34,35] and in the Algoryx Hydrodynamics module documentation [49], as well as in the OSC [48] software implementation. In addition, no wind loads are considered in the current model as we focus on evaluating the influence of wave loads on the system dynamics under regular waves. Consequently, the heave and pitch DOF are evaluated with respect to the turbine's COG located at 56 [m] from the base and a pitch radius of gyration of 69 [m] in the following sections (see Table 1 for further physical information about the model).

3 Methodology

The study of the FOWT concept described in this paper is based on its heave and pitch nonlinear hydrodynamic responses that were evaluated under regular wave conditions. These are computed using the Marine Simulator for two sets of *"Low Sea States"* and

Table 1 Physical properties of the components making up the T-Omega Wind FOWT shown in Fig. 1a

Ref.	Body	Mass abbreviation	Mass [t]	Dimensions [m]
1	Floating structure	m_f	503.8	Floats: 7x9.4 (radius and depth)
2	Tower	m_t	296.2	70x70x116 (in x, y and z)
3	Generator	m_g	140	8x3x1 (OR, IR and depth)
4	3-bladed rotor	m_b	60	69 (radius of gyration)

"High Sea States", with wave heights of $H \in [1-2]$ and $H \in [4-10]$ [m], respectively. For all cases, the range of wave periods considered spans across $T \in [3-25]$[s]. The accuracy of the model has been validated in our previous work [34] with the comparison of time-domain computed RAOs from the Marine Simulator time histories at each wave height case with the RAO responses evaluated from the experimental data. Experiments were performed through a series of tests of a scaled 1:60 prototype, conducted at the Kelvin Hydrodynamics Laboratory at the University of Strathclyde. RAOs evaluated from simulation results followed the procedure explained in [34], where turbines' RAOs in each DOF are obtained as the relation between the averaged maximum amplitude of turbines' responses and the excitation wave amplitude, such as $RAO \approx A^*_{[a]}/A_{[wave]}$; $A^*_{[a]}$ denoting the averaged amplitude of each DOF and A_{wave} is the wave excitation amplitude. In addition, the system's RAOs have been approximated using analytical expressions for each *Sea State*, expressed in Eqs. 6, 7 and 8 with detailed parameters given in Table 2 and are used as the reference RAOs for this study. In Fig. 2 the RAO approximations for heave and pitch displacements are depicted for *"High"* (black dashed line) and *"Low"* (blue dashed line) *Sea States*, alongside experimental data points obtained within the studied wave period range for wave heights of $H = 1$ and 2 [m] (stars) and $H = 4, 6, 8$ and 10 [m] (dots). Hence, the analytical RAO approximations can be evaluated as follows,

$$Heave\ RAO\ (T) = \begin{cases} \frac{2A/\pi b'}{1+4\left[\frac{T-X_o}{b'}\right]^2} + e \ \ \forall \ \ T \leq R \\ ln(T-f)d + c \ \ \forall \ T > R \end{cases}, \tag{6}$$

$$Pitch\ RAO\ (T) = \frac{2A/\pi b'}{1+4\left[\frac{T-X_o}{b'}\right]^2} + e\ , \tag{7}$$

where b' is evaluated with Eq. (8),

$$b' = \frac{2b}{1+exp\left\{\alpha(T-X_o)\right\}}\ . \tag{8}$$

In the above expressions R is the identified resonance period and T denotes the period of the wave excitation. A represents the non-dimensional area underneath the Lorentzian fit of the heave equation up to the resonance period R, while X_o is the non-dimensional centre of the Lorentzian maximum peak. In addition, α, b, c, d, e and f are the non-dimensional coefficients used for calibrating the RAO model.

FOWT dynamical simulations are performed for discrete wave excitation parameters within the specified range of the study and evaluated for both *"Low Sea States"* and *"High Sea States"*. Heave and pitch displacement time histories from the floating structure's CoG are recorded from the Marine Simulator computations and velocity time histories are computed with the time differential from the Marine Simulator displacement solutions. Finally, the turbines' velocities are evaluated from fitted sine series of order between 6th and 8th, which allows to analyse the system harmonics. This study focuses on the heave and pitch DOF dynamics only, as a result of the wave excitation nature (regular and advancing front parallel to the axis of gyration), which does not induce significant motion on the resting 4 DOF (previously observed in the wave tank experiments). The phase planes, Poincaré sections and FFT analysis are computed for selected discrete wave excitation parameters to evaluate system dynamics, natural frequencies and classify the type of periodic responses observed. The threshold between the types of periodic responses is approximated when varying the wave excitation period for a defined wave height, so that estimates the dominant solution can be obtained. An exemplary period-2 solution is shown in Fig. 3 for a wave excitation of $H = 6$[m] and period of $T = 4.81$[s], where panels (a) and (c) present the heave and pitch time histories, while panels (b) and (d) depict the velocity time histories for heave and pitch

Table 2 Heave and pitch analytical approximation parameters adjusted with experimental data for *"Low"* and *"High" Sea States* (Eqs. 6, 7 and 8)

Heave RAO [m/m]			Pitch RAO [deg/m]		
Parameter	*"Low Sea State"*	*"High Sea State"*	Parameter	*"Low Sea State"*	*"High Sea State"*
A	25.2	9.3	A	26.0	24.4
X_o	5.8	6.8	X_o	10.0	10.7
e	−0.95	−0.30	e	0.20	0.20
b	8.0	5	b	7.9	10.8
α	0.25	0.10	α	−0.15	−0.12
f	8.999	9.637	R	9.5	10.0
d	0.257	0.414			
c	0.292	0.217			

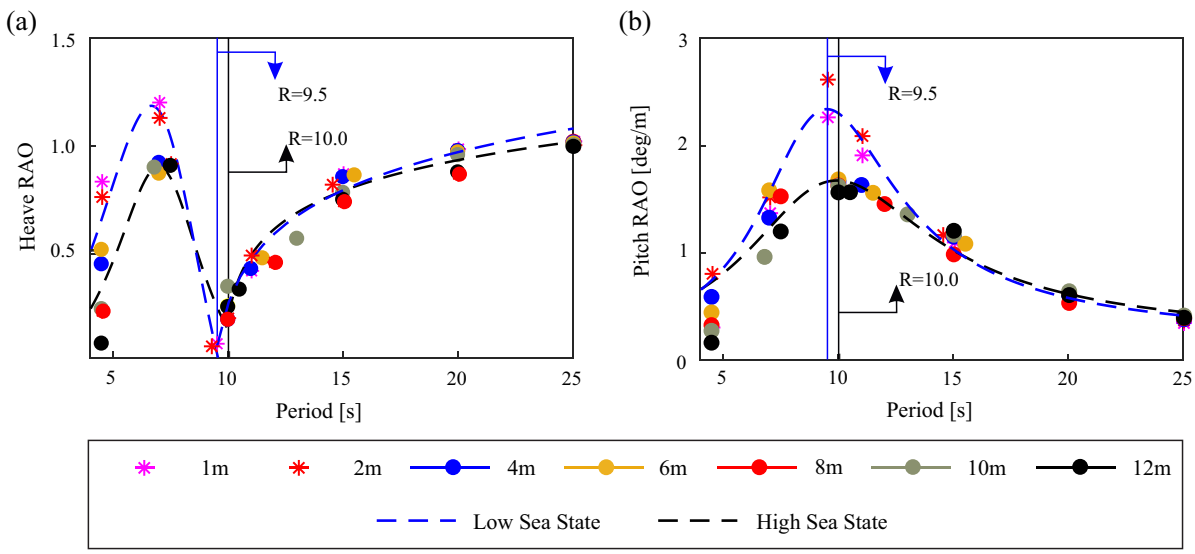

Fig. 2 Approximation of RAO responses evolution for wave periods of $T \in [4.5 - 25]$[s] and wave heights of $H \in [1 - 2]$ [m] for *"Low Sea States"* (dashed blue line) and $H \in [4-10]$ [m] for *"High Sea State"* (dashed black line). Dot and star markers show available experimental data used for the RAO approximations and R denotes the pitch resonant period for both cases. **a** Heave RAO responses. **b** Pitch RAO responses. [Adapted from: [34]]

response. The velocity time histories are approximated with a sum of sines series up to the 8th order in the form of Eq. 9,

$$d = \sum_{i=1}^{n=8} \Gamma_i sin\left(\Omega_i t + \Phi_i\right), \tag{9}$$

where d is the vertical velocity in $[m/s]$ or angular velocity in $[deg/s]$ and Γ_i, Ω_i and Φ_i denote the amplitude, frequency and phase constant for i-th sinusoidal terms.

Phase planes and Poincaré sections (red dots) for both DOFs are shown in Fig. 3, panels (e) and (g), which present examples of period-2 oscillation responses. The response frequencies are evaluated using the FFT analysis and depicted in panels (f) and (h) for heave and pitch displacements, respectively. These show at 0.101 [Hz] the FOWT's frequency response for both heave and pitch, and at 0.208 [Hz] the wave excitation frequency for the case presented in Fig. 3, which indicates period-2 solution. In the same manner, period-1, period-2 and period-3 responses can be identified

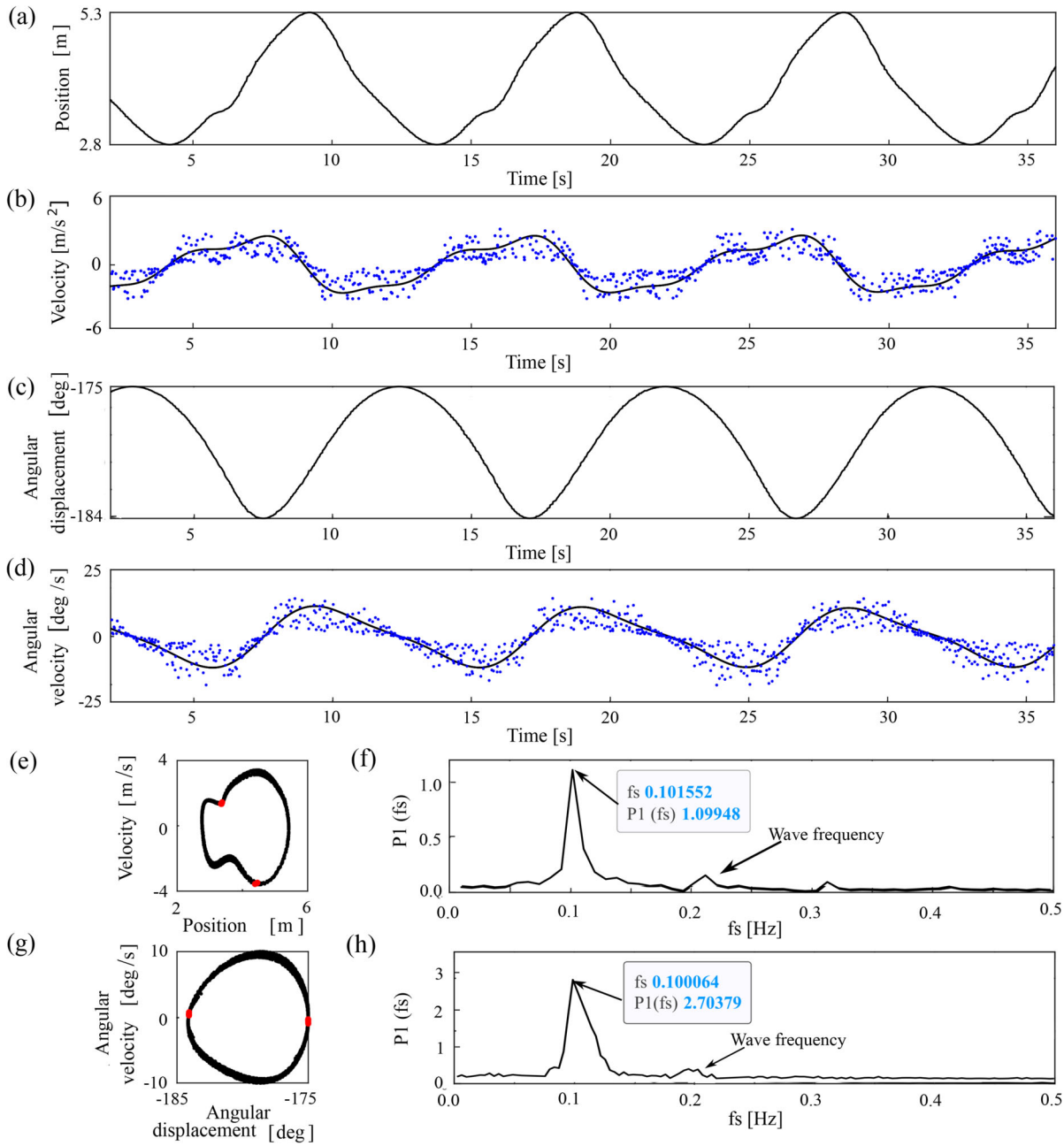

Fig. 3 Example simulation results showing evaluation of a period-2 response for the FOWT concept under regular wave excitation of $H = 6$[m] and $T = 4.81$[s]. **a** Heave displacement time history and **b** corresponding heave velocity time history. **c** Pitch angular displacement time history and **d** corresponding time history of pitch angular velocity. Velocity time histories represent in blue dots the actual computed differential solution and the black continuous line is the approximated system velocity response. **e** Heave phase plane and Poincaré section (red dots) showing a period-2 response and **f** corresponding FFT plot for heave displacement showing a fundamental frequency at 0.101552 [Hz]. **g** Pitch phase plane and Poincaré section (red dots) showing a period-2 system's response and **h** corresponding FFT plot for pitch angular displacement showing a fundamental frequency at 0.101587 [Hz]. (Wave frequency at 0.207900 [Hz])

for the range of wave parameter values stated above (See Figs. 6 and 7). An example of period-3 response is presented for wave excitation of $H = 8$[m] and $T = 3.76$[s] in Appendix A.

Such analysis allows us to investigate the nonlinear response of the design and understand the evolution of the phase planes as the wave period increases for a given wave height. The next section presents the evaluation of dynamical behaviour of the T-Omega Wind system under wide range of hydrodynamical loading.

4 Results and discussion

The dynamic behaviour and frequency responses of the T-Omega Wind FOWT concept are investigated numerically under regular wave influence with simulations performed in the Marine Simulator. The excitation waves impinge on the turbine with a wave advancing front of direction parallel to its rotation axis. Hence, the concept is evaluated in its current design configuration using the experimentally calibrated numerical model. Previous studies [34] validating the RAO responses of the system and subsequent simulations presented in this work, predict a strong coupling between the heave and pitch DOFs, which is demonstrated by the pitch maximum displacement coinciding with the heave minimum displacements for all considered sea states (see Fig. 2). Hence, cross-sectional trajectories depicting the coupling between heave and pitch displacements are evaluated showing that at pitch resonance period ($T \in [9.5 - 10.0]$[s]) the heave displacement does not surpass the 3.6 [m] of displacement amplitude for the highest wave height considered, $H = 10$[m]. A selection of cross-sectional trajectories are depicted in Fig. 4 for representative wave excitation periods close to the pitch resonance period for wave heights of $H = 4$[m] (Fig. 4a–d) and $H = 6$[m] (Fig. 4d–h). The results topology show that close loops become narrower as the excitation period gets closer to the pitch resonance, depicting the significant decrease in heave displacement and the topology stabilization as the excitation period moves away from it. The latter observation aligns with previous findings by Amaral et al. [41], who showed that coupling is particularly evident for large floating structure angular displacements. Moreover, the force cancellation effect generated by the floats spacing minimize the vertical motions as previously reported by Nihei et al. [50] and in Wang et al. [51] for this particular case. Results referring to surge, sway, roll and yaw DOF are neglected in this paper since solutions are close to zero values.

This study focuses on the wave parameter ranges and thresholds identification for different types of periodic responses that the FOWT exhibits at a given wave height and wave frequency. Thus, simulations are performed for ranges of discrete wave period values between $T = [3 - 25]$[s] with precision of ± 0.01[s] and selected phase planes, Poincaré sections, time histories and FFT responses are evaluated with a custom developed Matlab script to investigate in detail the FOWT's dynamical behaviour. The results show that for *Low Sea States* ($H = [1 - 2]$ [m]) period-1 oscillations are dominant in the direction of the incident wave for all wave frequencies ($T \in [3 - 25]$[s]) [22,52,53]. For that case nearly linear heave and pitch turbine responses are observed for wave periods greater than $T > 12$ [s] and $T > 13$[s] for $H = 1$ and $H = 2$[m], respectively. This is due to only observing the fundamental frequency for both degrees of freedom. For lower periods of wave excitation between approximately $T \in [3 - 10]$[s] up to the $4th$ harmonic can be identified for the heave responses, in contrast with the corresponding pitch responses, which show a nearly linear response. The former situation is clearly identified for low periods of wave excitation close to the pitch resonance period ($T_R = 10$[s]) and its neighbouring periods, such as for example the case of $H = 2$[m] and $T = 10.2$[s]. Thus, up to $4th$ harmonic can be clearly observed for heave responses, whereas pitch response only exhibits its fundamental frequency, as shown in the FFT analysis of Fig. 5f. The nonlinearities identified in the system responses, which introduce the nth harmonics to the response are attributed to the geometrical nonlinearities induced by the conical-cylindrical floats shape. Since the FOWT waterline is variable when the heave response is large, the wave height and period will influence the rate of its variation, making those nonlinearities more noticeable for higher wave heights and particularly for lower wave periods.

In coherence with previous results shown above, the FOWT periodic type responses are investigated in *High Sea States* for discrete wave heights of $H = [4, 6, 8, 10]$ [m] within the wave period domain of $T \in [3.00 - 25.00]$ [s] resulting in the identification of period-1, periods-2, period-3 and period-4 type solutions, where the latter is only observed for wave heights of $H = 4$[m]. For all cases considered, period-

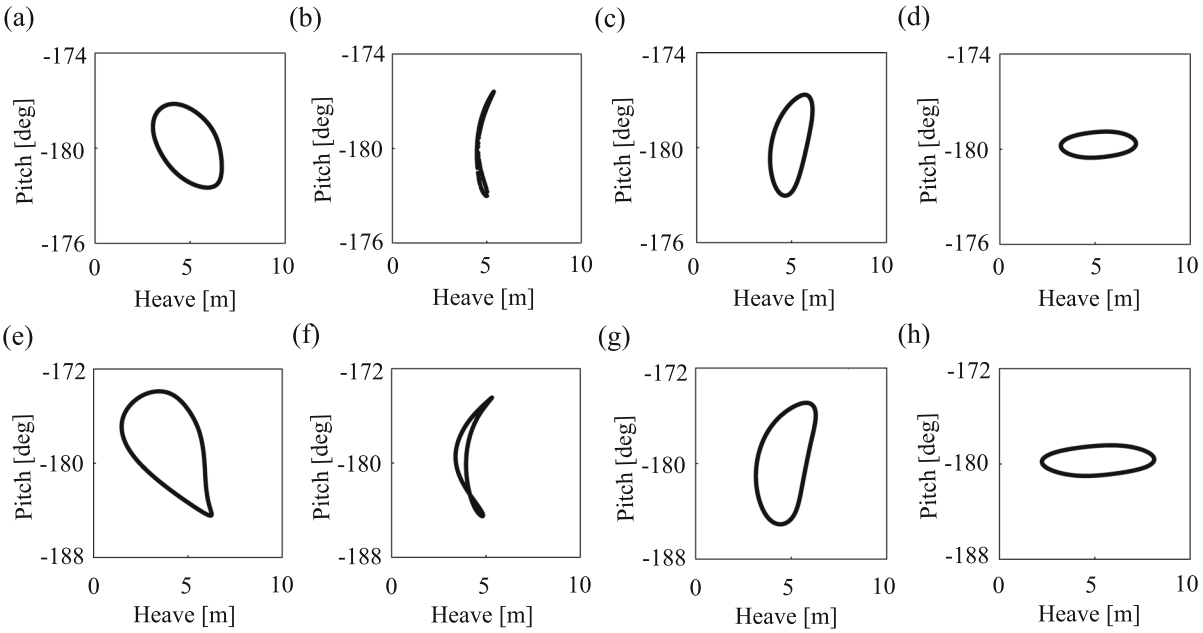

Fig. 4 Heave and pitch displacement correlation for selected values of wave height and period showing the cancelling effect at pitch resonance period of $T = 10[s]$ for *"High Sea State"* cases. **a**–**d** Wave height of $H = 4$[m] and from left to right with ascending periods of $T = [8.00, 10.00, 12.00, 14.00]$[s] respectively; and **e**–**h** wave height of $H = 6$[m] and from left to right with ascending periods of $T = [7.50, 10.00, 12.00, 14.00]$[s] respectively

1 solutions exist for excitation periods greater than the system's resonance period of $T = 10$[s], whereas the existence of this type of responses below the pitch resonant period threshold vary depending on the excitation wave height. An example of results obtained for the FOWT dynamical responses under wave height of $H = 6$[m] is presented in Fig. 6a, where the response types are marked in yellow, green and blue regions depicting period-1, period-2 and period-3 responses, respectively. Period-1 responses are identified for ranges of wave excitation periods larger than $T > 6.80$[s], period-2 responses exist within the range of $T \in [4.49 - 6.80]$[s] and period-3 oscillations are identified for periods within the range of $T \in [3.00 - 4.49]$[s]. Selected phase planes and Poincaré sections show the topology of the responses and the periodicity identified. For this case, no discrepancies between heave and pitch period-type responses are identified and for larger wave excitation periods of $T \geq 15.00$[s] only first order harmonic responses are obtained. In addition, Fig. 6b and c depict the phase plane evolution for heave and pitch DOF, respectively. Hence, larger displacements and velocities are observed for both resonant periods at $T = 7$[s] and $T = 10$[s] for heave and pitch, respectively. At this point, the nonlinearities induced by the rapid change in the float's waterline is evident in the phase planes depicting the visible folds.

Regions of periodic-type responses vary and it can be concluded that the region where period-1 responses dominate for heave and pitch reduces as the wave height increases. Moreover, for wave height of $H = 4$[m], period-4 oscillations can be observed for both DOF between excitation periods of $T \in [3.0 - 3.6]$[s] evolving into period-2 solutions through a period halving bifurcation at approximately $T = 3.6$[s]. In addition, period-2 oscillations are present between $T \in [3.6 - 4.5]$[s] and preferable period-1 solutions are observed for wave excitation periods greater than $T > 4.5$[s]. Moreover, for wave heights bigger than $H \geq 6$[m], all considered cases depict similar period-type responses as for the previously described case of $H = 6$[m] with similar nonlinear behaviours identified when reaching the resonant heave and pitch periods. Note that, period-3 and period-2 type solutions exist for wider ranges of wave period when the wave height is increased. Thus, narrowing the range of wave periods, where period-1 solution exists and expanding regions where less desirable responses can occur. For wave heights of $H = 8$[m], period-3 oscillations are identified for $T \in [3.00 - 4.00]$[s] and period-2 for $T \in [4.00 - 5.90]$[s].

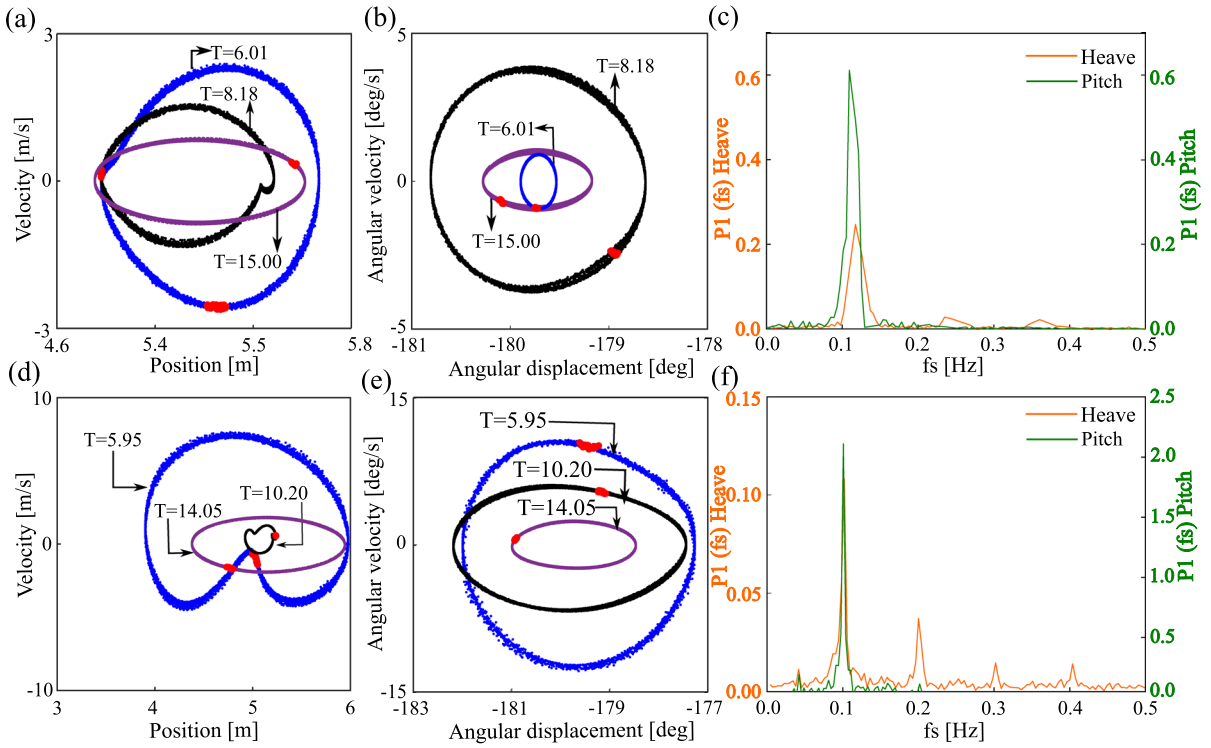

Fig. 5 Selection of *"Low Sea States"* phase planes, Poincaré sections (red dots) FFT analysis for heave and pitch displacements showing period-1 turbine responses. Blue, black and purple colours depict heave and pitch phase planes for selected periods in ascending order **a**–**b** Heave and pitch phase planes and Poincaré sections for wave height of $H = 1$[m] and wave periods of $T = [6.01, 8.18, 15.00]$[s] depicted in blue, black and purple, respectively. **c** FFT analysis for heave and pitch displacements depicted in orange and green for the case of $H = 1$[m] and $T = 8.18$[s] showing fundamental frequencies and up to 3^{rd} harmonic for heave displacements. **d**–**e** Heave and pitch phase planes and Poincaré sections for wave height of $H = 2$[m] and wave periods of $T = [5.95, 10.20, 14.05]$[s] depicted in blue, black and purple, respectively. **f** FFT analysis for heave and pitch displacements depicted in orange and green colours for the case of $H = 2$[m] and $T = 10.20$[s] showing fundamental frequencies and up to $4th$ harmonic for heave displacements

In addition, for $H = 10$[m] period-3 solutions exist within range of $T \in [3.00-4.80]$[s] and period-2 when $T \in [4.80 - 6.5][s]$. Figure 7 summarizes the variety of types of periodic responses observed under different wave heights and wave periods. These are depicted as colour-shadowed striped regions represented over the turbine RAO responses for heave and pitch displacements. Shadowed regions in red, blue, green and yellow denote period-4, period-3, period-2 and period-1 oscillatory responses, respectively. It is observed that for *"High Sea States"* at regions of very low excitation periods ($T < 5[s]$), all cases depict a wide variety of higher order of periodic orbits and the period type response variations are highly sensitive to wave height fluctuations. This can be related to the greater heave and pitch displacement variation, when wave height changes. This is showed in Fig. 2 with scattered RAO responses for both DOF in the aforementioned wave periods. To visualise the evolution of the possible system responses, Fig. 8 presents the heave and pitch phase planes as a function of wave period (selected cases to visualise variety in phase planes). These confirm the initial prediction that for wave periods greater than $T = 15[s]$, the responses are dominantly period-1 oscillations and small nonlinearities are visible in the responses. Note that period-1 solution of simple harmonic motion nature can be encountered in heave and pitch when RAOs are close to 1. This indicates that floats almost maintain an invariant waterline under regular wave excitations. Hence, presenting ideal conditions when the FOWT glides over waves, following them directly.

The FFT analysis conducted for selected cases of *"High Sea States"* indicates that for excitation periods below

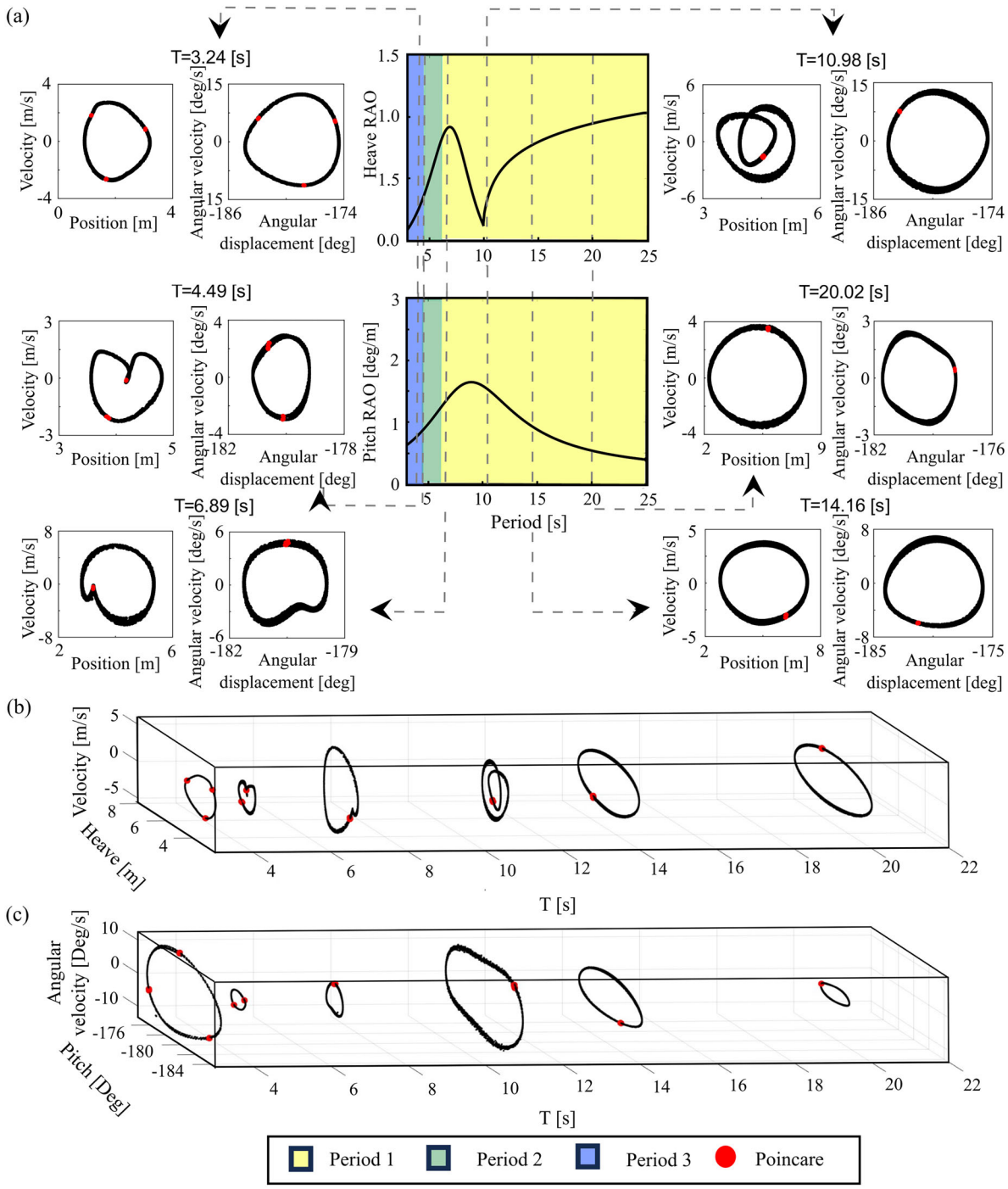

Fig. 6 Evolution of system dynamics for heave and pitch DOFs under regular wave excitation: $H = 6$[m] and $T \in [3-25]$[s]. **a** Analytical heave and pitch RAO prediction for *"High Sea States"* with regions where period-1, period-2 and period-3 solutions (marked in yellow, green and blue) were observed for $H = 6$[m]. Selected phase planes for both DOFs showing the variety of responses and their Poincaré sections for specific wave periods are shown in panels surrounding RAO plots. **b–c** Evolution of phase for heave and pitch showing the type of system responses and corresponding Poincaré

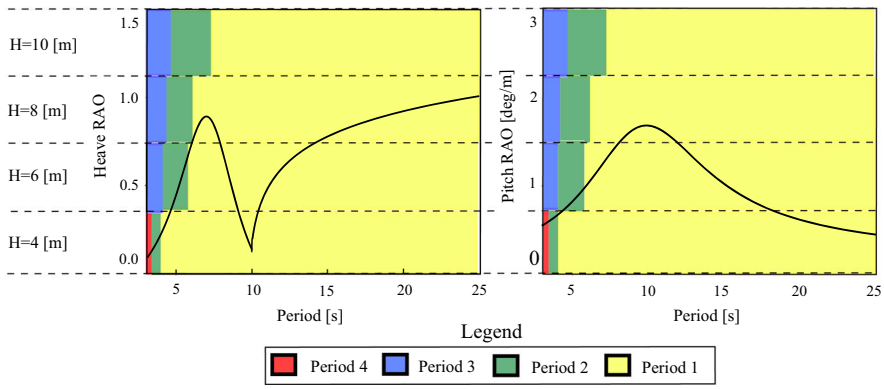

Fig. 7 Parametric plot showing type of responses and their evolution dependent on regular wave excitation parameters (wave height and period) for *"High Sea States"*, where $H = 4, 6, 8$ and 10[m] and $T \in [3 - 25]$[s]. Period-1, period-2, period-3 and period-4 are marked in yellow, green, blue and red, respectively

the pitch resonant value the system response contains harmonics of order between $4th$ and $7th$, that occur for both heave and pitch DOF. However, when closer to the pitch resonance period, heave responses display the $4th$ order harmonics, whereas pitch identified harmonics vary between $2nd$ and $4th$ order depending on the wave height in the range considered, $H \in [4 - 10]$[m]. For some cases, the $2nd$ order harmonic is the dominant frequency when the forcing frequency is close to the pitch resonance. This effect has previously been identified for a semi-submersible floating structure by Hansen et al. [54], where the pitch resonance is driven by the pitch second-order even harmonic.

In addition, for *"High Sea States"*, when the excitation period is greater than the pitch resonant period (i.e. $T > 14$[s], close to heave $RAOs \sim 1$) both DOF present the fundamental frequency. This permits the assumption of linear responses with the exception of wave heights of $H = 10$[m] and $T > 20$[s], where $2^{nd} online$ harmonics become visible for pitch oscillations.

The nonlinearities in the FOWT responses are identified for both heave and pitch displacements and depicted in the motion time histories and phase planes. These are induced by the geometry nonlinearities in the floats, the variation of waterline on them and the variation of viscous damping [55]. These are especially visible when the floating system does not accurately glide over sea waves and the waterline variation is greater. Thus, from the wave parameters investigated, these behaviours are specifically profound for heave displacements considerably smaller than the wave height ($RAO\,Heave << 1$). This is specially visible for small wave periods within interval $T \in [3 - 6]$[s] and for wave periods close to the pitch resonance. Both cases can be identified from the folds and overall topology of phase planes for heave and pitch. In cases of small wave periods the folds depicting nonlinearities are not clearly visible, as in Fig. 8 due to the small FOWT displacements and velocities.

Nevertheless, close to the pitch resonant period they are clearly observable in the heave phase planes shown in Fig. 8a, c, e, for $H = 4$[m] and $T = 10$[s], $H = 8$[m] and $T = 7.00$[s] and $H = 10$[m] and $T = 12.92$[s], respectively. In contrast, pitch does not show such as a strong nonlinear nature since for most cases, the time histories are closer to linear responses. An example of heave induced nonlinearity is shown in Fig. 6a for wave excitation period of $T = 10.98$[s]. In addition, the RAO responses of heave and pitch displacements for *"Low"* and *"High" Sea States* show the existence of a high coupling effect between both DOF, since the pitch resonant period coincides with the wavelength of minimum heave displacement. This effect has been previously reported by Nagumo et al. [55], who showed that light FOWTs present this behaviour due to a single mooring line. Moreover, roll and surge displacements have been neglected in this study since no displacements have been observed in the experimental results presented for this wind turbine concept in [34] and previous studies [55] for a similar concept, which does not suggest a strong coupling between the considered displacements and the roll.

5 Concluding remarks

This paper investigated numerically the heave and pitch dynamic responses of a new type of shallow-draft FOWT concept under regular wave excitations for both *"Low"* and *"High" Sea States*. A multibody virtual

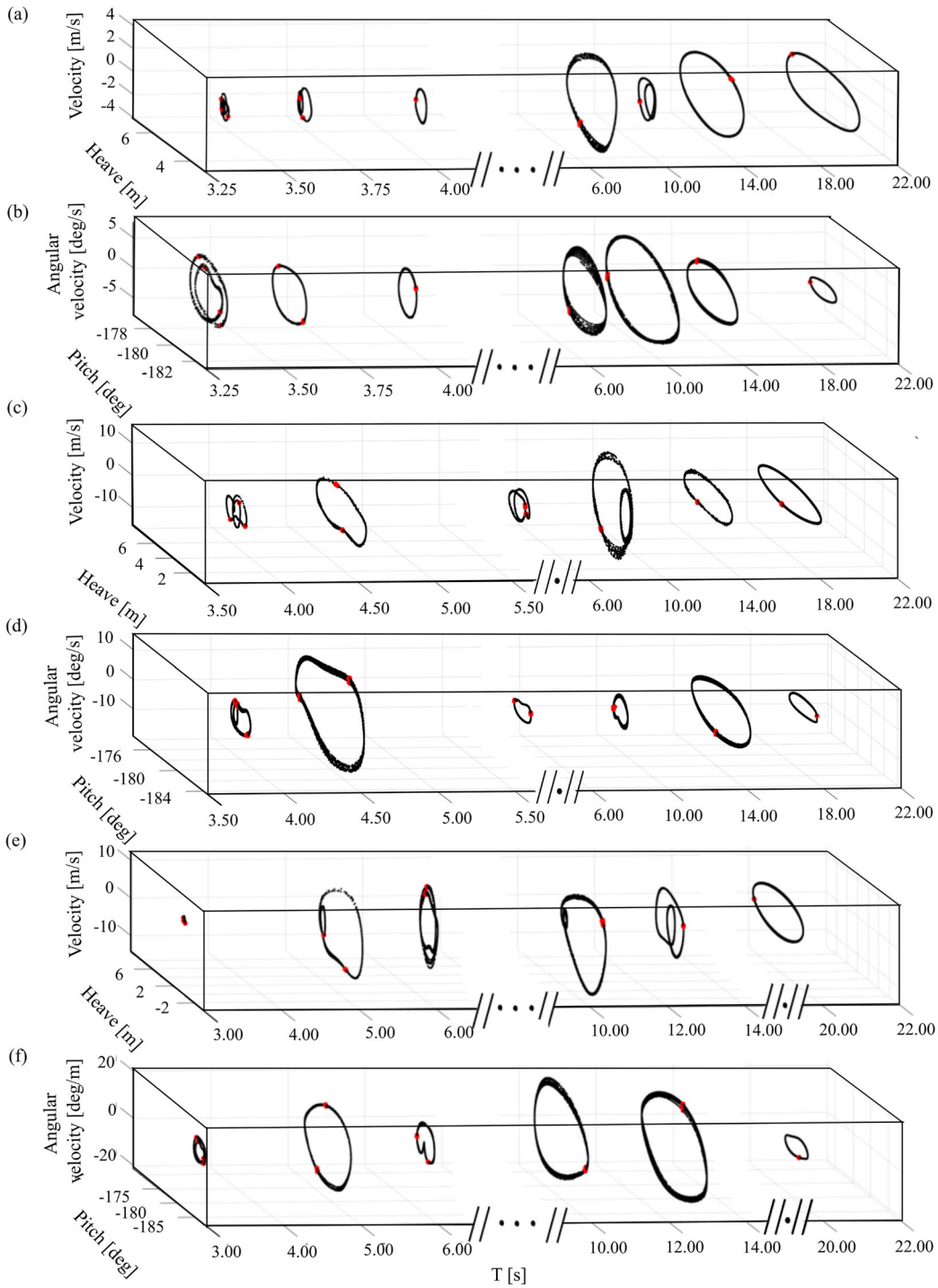

Fig. 8 Evolution of system dynamics and phase planes for heave and pitch DOFs under regular wave excitation for $T \in [3 - 25][s]$ showing the type of system responses and corresponding Poincaré section for **a**, **b** $H = 4[m]$, **c**, **d** $H = 8[m]$ and $H = 10[m]$. (Refer to Fig. 6 for evolution of H=6[m])

model that has been simplified to a 6 DOF model with high stiffness couplings and previously validated with a 1:60 scaled prototype wave tank experiments is implemented in the state-of-art real-time Marine Simulator. The simulation results proved that the turbine presents dominant period-1 responses within the frequency domain studied for both *Sea States*. The periodic responses observed for the wind turbine under hydrodynamic loading are classified by its periodicity and ranges where each solution dominates and are clearly identified within the considered wave height $H \in [1-10]$[m], and wave period $T \in [3-25]$[s], intervals. Heave and pitch time histories, phase planes and Poincaré sections show that period-1 responses are observed for *"Low Sea States"* and up to period-4 heave responses are observed for *"High Sea States"* for smaller wave periods. The ranges of periodic response types depend on the excitation wave height and are defined in this paper for every considered wave height and period between $T \in [3-25]$[s]. Period-1 solutions are observed for wave periods greater than the turbines' resonant period ($T_R = 10$[s]) for all wave height cases studied. Hence, period-1 oscillations exist for wave excitation periods within $T \in [10-25]$[s]. This proves that for the most common sea states the considered FOWT design is able to glide over sea waves with period-1 responses.

The model's nonlinearities for heave and pitch displacements are identified for all cases studied, observing stronger nonlinear responses for cases when the turbine is subjected to *"High Sea State"* scenarios, which is caused by the nonlinearities induced by the geometry of the conic-circular shaped floats. This change in geometry induces a variation in the viscous damping generated by the change in the float's waterline. This effect is more prominent as the wave height increases and for lower wave periods. FFT analysis in conjunction with previous studies is used to identify the frequencies present in the system responses, concluding that more prominent nonlinear responses are captured when heave RAOs are considerably below 1, $Heave\,RAO << 1$ (relative structure elevation less than wave elevation). For cases of small wave height, $H \in [1-2]$[m] (*"Low Sea States"*), up to $4th$ order harmonics are identified for heave responses, while pitch responses present only the fundamental frequency for shorter wave excitation periods. In contrast, for *"High Sea States"* the same nth order harmonics are visible for both DOF and higher harmonics are identified only for small periods of excitation, which are less common in a deep-water sea environment. Finally, the coupling between heave and pitch DOFs is demonstrated though the period-type evolution, where for most cases both DOFs depict the same type of periodicity. In addition, the heave RAO decreases coinciding with the pitch resonant period, showing a heave RAO minimum for the pitch RAO maximum. Hence, this evidences that coupling evaluation is required to accurately evaluate the system dynamics. In line with those results, it is suggested that the next line of research should include the gyroscopic effect of the turbine to evaluate the dynamics of the turbine under combined wave and wind loading. This will permit further advancement of the considered FOWT concept.

Acknowledgements The authors wish to thank T-Omega Wind Inc. for their support towards this project.

Author contributions AT-G: Writing- original draft, Methodology, Formal analysis, Investigation and Visualisation. SD: Investigation, Resources and Writing—review & editing. RDN: Funding acquisition, Writing—review & editing. JP: Resources, Writing—review & editing. MK: Supervision, Project administration, Conceptualization, Visualisation, Funding acquisition and Writing—review & editing.

Funding This work has benefited from the support and funding received from Net Zero Technology Centre and The University of Aberdeen through their partnership in The National Decommissioning Centre (NDC) and The Scottish Government's Decommissioning Challenge Fund in part-funding the establishment of the Marine Simulator research facility at the NDC.

Data Availibility Statement Data will be made available on request.

Declarations

Conflict of interest The four university-employed authors declare that they have no known competing financial interests or personal relationships that could have appeared to influence the work reported in this paper. Jim Papadopoulos, co-founder and Chief Engineer of T-Omega Wind, served as a manuscript

reviewer/editor and did not otherwise influence the investigation or the presentation of results.

Appendix A Period-3 response

See Fig. 9.

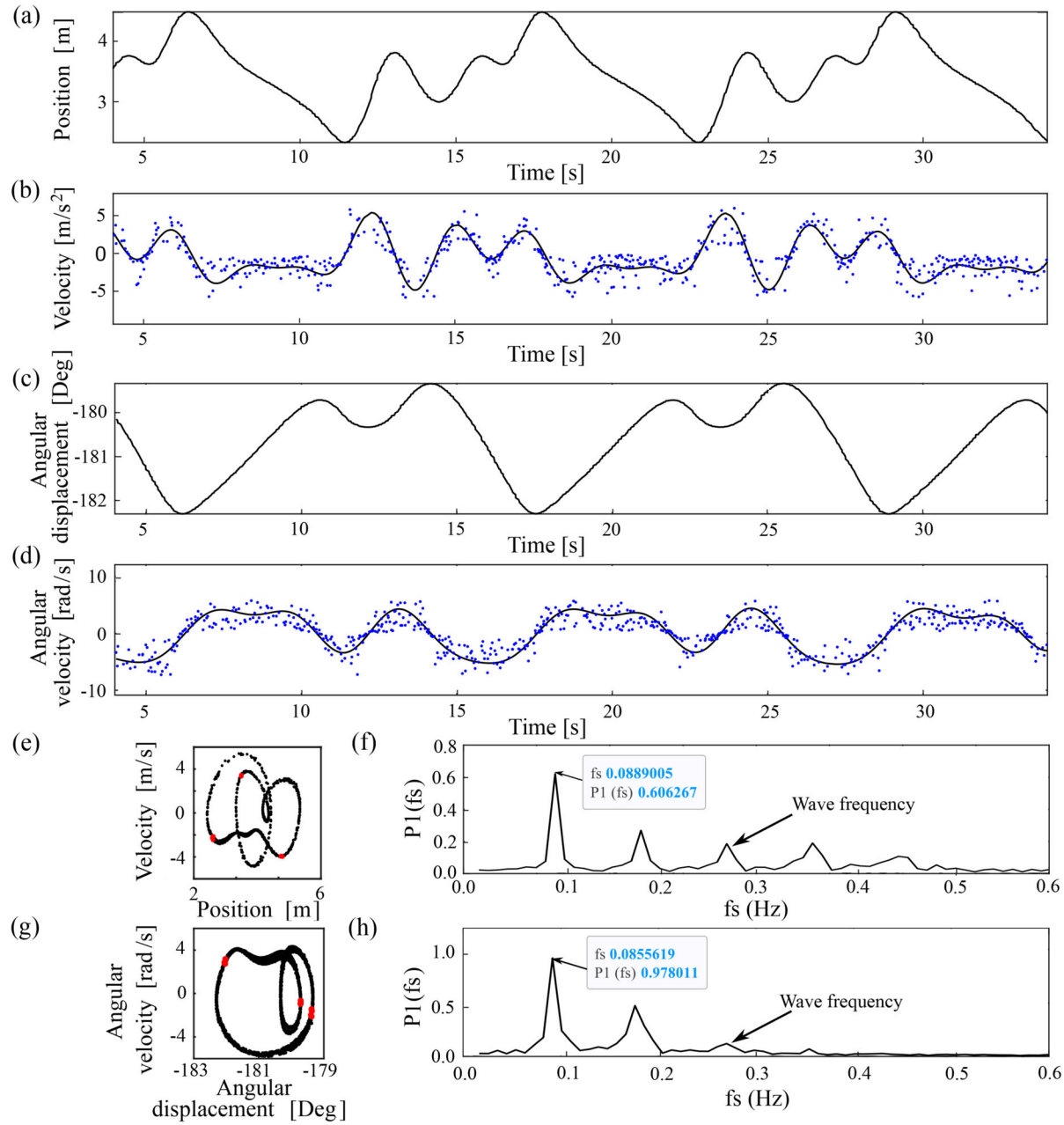

Fig. 9 Example simulation results showing evaluation of a period-3 response of the FOWT concept under regular wave excitation of $H = 8$[m] and $T = 3.76$[s]. **a** Heave displacement time history and **b** corresponding time history of heave velocity. **c** Pitch angular displacement time history and **d** corresponding time history of pitch angular velocity Velocity time histories represent in blue dots the actual computed differential solution and the black continuous line is the approximated system velocity response. **e** Heave phase plane and Poincaré section (red dots) showing a period-3 system's response and **f** corresponding FFT plot for heave displacement showing a fundamental frequency at 0.0.0889005 [Hz]. **g** Pitch phase plane and Poincaré section (red dots) showing a period-3 system's response and **h** corresponding FFT plot for pitch angular displacement showing a fundamental frequency at 0.0855619 [Hz]. (Wave frequency at 0.2667020 [Hz])

References

1. Ghigo, A., Faraggiana, E., Giorgi, G., Mattiazzo, G., Bracco, G.: Floating vertical axis wind turbines for offshore applications among potentialities and challenges: a review. Renew. Sustain. Energy Rev. **193**, 114302 (2024)
2. Nytte, S., Alfnes, F., Korhonen-Sande, S.: Public support and opposition toward floating offshore wind power development in Norway. Electr. J. **37**, 107336 (2024)
3. Gomes, J.G., Lin, Y., Jiang, J., Yan, N., Dai, S., Yang, T.: Review of offshore wind projects status: New approach of floating turbines. In: 2022 5th International Conference on Power and Energy Applications (ICPEA), pp. 676–686 (2022)
4. Ibrion, M., Nejad, A.R.: On a road map for technology qualification, innovation and cost reduction in floating offshore wind: learning from Hywind and Norwegian approach. In: Journal of Physics: Conference Series, vol. 2507, p. 012008 (2023). IOP Publishing
5. Edwards, E.C., Holcombe, A., Brown, S., Ransley, E., Hann, M., Greaves, D.: Trends in floating offshore wind platforms: a review of early-stage devices. Renew. Sustain. Energy Rev. **193**, 114271 (2024)
6. Terrero Gonzalez, A., Dunning, P., Howard, I., McKee, K., Wiercigroch, M.: Is wave energy untapped potential? Int. J. Mech. Sci. **205**, 106544 (2021)
7. Micallef, D., Rezaeiha, A.: Floating offshore wind turbine aerodynamics: trends and future challenges. Renew. Sustain. Energy Rev. **152**, 111696 (2021)
8. Zeng, X., Shao, Y., Feng, X., Xu, K., Jin, R., Li, H.: Nonlinear hydrodynamics of floating offshore wind turbines: a review. Renew. Sustain. Energy Rev. **191**, 114092 (2024)
9. Zhang, H., Wang, H., Cai, X., Xie, J., Wang, Y., Zhang, N.: Novel method for designing and optimising the floating platforms of offshore wind turbines. Ocean Eng. **266**, 112781 (2022)
10. Kim, K., Kim, H., Kim, H., Son, J., Kim, J., Park, J.: Resonance avoidance control algorithm for semi-submersible floating offshore wind turbine. Energies **14**(14), 4138 (2021)
11. Papi, F., Bianchini, A., Ferri, G., Bruschi, N., Marino, E.: Influence of tower design on floating offshore wind turbine dynamics. In: International Conference on Offshore Mechanics and Arctic Engineering, vol. 8: Ocean Renewable Energy, pp. 008–09053 (2023)
12. Luo, Y., Qian, F., Sun, H., Wang, X., Chen, A., Zuo, L.: Rigid-flexible coupling multi-body dynamics modeling of a semi-submersible floating offshore wind turbine. Ocean Eng. **281**, 114648 (2023)
13. Bagherian, V., Salehi, M., Mahzoon, M.: Rigid multibody dynamic modeling for a semi-submersible wind turbine. Energy Convers. Manage. **244**, 114399 (2021)
14. Al-Solihat, M.K., Nahon, M.: Flexible multibody dynamic modeling of a floating wind turbine. Int. J. Mech. Sci. **142**, 518–529 (2018)
15. Al-Solihat, M.K., Nahon, M., Behdinan, K.: Dynamic modeling and simulation of a spar floating offshore wind turbine with consideration of the rotor speed variations. J. Dyn. Syst. Meas. Contr. **141**(8), 081014 (2019)
16. Jonkman, J.M.: Modeling of the UAE wind turbine for refinement of fast AD. Technical report, National Renewable Energy Lab.(NREL), Golden, CO (United States) (2003)
17. Larsen, T.J., Hansen, A.M.: How 2 HAWC2, the user's manual. RisøReport, Risø **702** (2009)
18. Bossanyi, E.: GH bladed theory manual. GH & Partners Ltd **2**, 56–58 (2003)
19. Takata, T., Takaoka, M., Gonçalves, R.T., Houtani, H., Yoshimura, Y., Hara, K., Oh, S., Dotta, R., Malta, E.B., Iijima, K., et al.: Dynamic behavior of a flexible multicolumn FOWT in regular waves. J. Mar. Sci. Eng. **9**(2), 124 (2021)
20. Wang, L., Sweetman, B.: Simulation of large-amplitude motion of floating wind turbines using conservation of momentum. Ocean Eng. **42**, 155–164 (2012)
21. Lee, D., Hodges, D.H., Patil, M.J.: Multi-flexible-body dynamic analysis of horizontal axis wind turbines. Wind Energy Int. J. Progr. Appl. Wind Power Convers. Technol. **5**(4), 281–300 (2002)
22. Subbulakshmi, A., Verma, M., Keerthana, M., Sasmal, S., Harikrishna, P., Kapuria, S.: Recent advances in experimental and numerical methods for dynamic analysis of floating offshore wind turbines-an integrated review. Renew. Sustain. Energy Rev. **164**, 112525 (2022)
23. Ha, Y., Kim, K., Park, J.: CFD study of the non-linear physical phenomena of the TLP of a 15-MW-class FOWT under extreme waves. J. Mar. Sci. Eng. **11**(10), 1915 (2023)
24. Zhou, Y., Xiao, Q., Liu, Y., Incecik, A., Peyrard, C., Li, S., Pan, G.: Numerical modelling of dynamic responses of a floating offshore wind turbine subject to focused waves. Energies **12**(18), 3482 (2019)
25. Antonutti, R., Peyrard, C., Johanning, L., Incecik, A., Ingram, D.: The effects of wind-induced inclination on the dynamics of semi-submersible floating wind turbines in the time domain. Renew. Energy **88**, 83–94 (2016)
26. Wang, Y., Chen, H.-C., Koop, A., Vaz, G.: Hydrodynamic response of a FOWT semi-submersible under regular waves using CFD: verification and validation. Ocean Eng. **258**, 111742 (2022)
27. Tran, T.T., Kim, D.-H.: The coupled dynamic response computation for a semi-submersible platform of floating offshore wind turbine. J. Wind Eng. Ind. Aerodyn. **147**, 104–119 (2015)
28. Zou, Q., Lu, Z., Shen, Y.: Short-term prediction of hydrodynamic response of a novel semi-submersible FOWT platform under wind, current and wave loads. Ocean Eng. **278**, 114471 (2023)
29. Xu, K., Shao, Y., Gao, Z., Moan, T.: A study on fully nonlinear wave load effects on floating wind turbine. J. Fluids Struct. **88**, 216–240 (2019)
30. Patryniak, K., Collu, M., Coraddu, A.: Rigid body dynamic response of a floating offshore wind turbine to waves: identification of the instantaneous centre of rotation through analytical and numerical analyses. Renew. Energy **218**, 119378 (2023)
31. Karimirad, M., Michailides, C.: V-shaped semi-submersible offshore wind turbine: an alternative concept for offshore wind technology. Renew. Energy **83**, 126–143 (2015)
32. Liu, B., Yu, J.: Dynamic response of spar-type floating offshore wind turbine under wave group scenarios. Energies **15**(13), 4870 (2022)

33. Zhao, Z., Shi, W., Wang, W., Qi, S., Li, X.: Dynamic analysis of a novel semi-submersible platform for a 10 MW wind turbine in intermediate water depth. Ocean Eng. **237**, 109688 (2021)
34. Terrero-Gonzalez, A., Dai, S., Neilson, R.D., Papadopoulos, J., Kapitaniak, M.: Dynamic response of a shallow-draft floating wind turbine concept: experiments and modelling. Renew. Energy **226**, 120454 (2024)
35. Martinez, R., Arnau, S., Scullion, C., Collins, P., Neilson, R.D., Kapitaniak, M.: Variable buoyancy anchor deployment analysis for floating wind applications using a marine simulator. Ocean Eng. **285**, 115417 (2023)
36. Tabeshpour, M.R., Shoghi, R.: Perturbation nonlinear response of tension leg platform under regular wave excitation. J. Mar. Sci. Technol. **23**, 132–140 (2018)
37. Alkarem, Y.R., Ozbahceci, B.: A complemental analysis of wave irregularity effect on the hydrodynamic responses of offshore wind turbines with the semi-submersible platform. Appl. Ocean Res. **113**, 102757 (2021)
38. Ramos, R.L.: Linear quadratic optimal control of a spar-type floating offshore wind turbine in the presence of turbulent wind and different sea states. J. Mar. Sci. Eng. **6**(4), 151 (2018)
39. Zeng, F., Zhang, N., Huang, G., Gu, Q., He, M.: Experimental study on dynamic response of a floating offshore wind turbine under various freak wave profiles. Mar. Struct. **88**, 103362 (2023)
40. Zeng, F., Zhang, N., Huang, G., Gu, Q., Pan, W.: A novel method in generating freak wave and modulating wave profile. Mar. Struct. **82**, 103148 (2022)
41. Amaral, G.A., Mello, P.C., Carmo, L.H., Alberto, I.F., Malta, E.B., Simos, A.N., Franzini, G.R., Suzuki, H., Gonçalves, R.T.: Seakeeping tests of a FOWT in wind and waves: an analysis of dynamic coupling effects and their impact on the predictions of pitch motion response. J. Mar. Sci. Eng. **9**(2), 179 (2021)
42. Tian, X., Xiao, J., Liu, H., Wen, B., Peng, Z.: A novel dynamics analysis method for spar-type floating offshore wind turbine. China Ocean Eng. **34**, 99–109 (2020)
43. Edwards, E.C., Holcombe, A., Brown, S., Ransley, E., Hann, M., Greaves, D.: Evolution of floating offshore wind platforms: a review of at-sea devices. Renew. Sustain. Energy Rev. **183**, 113416 (2023)
44. Ghabraei, S., Moradi, H., Vossoughi, G.: Investigation of the effect of the added mass fluctuation and lateral vibration absorbers on the vertical nonlinear vibrations of the offshore wind turbine. Nonlinear Dyn. **103**, 1499–1515 (2021)
45. Riyanto, R.D., Papadopoulos, J.M., Myers, A.T.: Numerical investigation of wave following mechanism of shallow draft floating wind turbine. In: International Conference on Offshore Mechanics and Arctic Engineering, vol. 86618, pp. 001–01017 (2022). American Society of Mechanical Engineers
46. Li, Y., Tang, Y., Zhu, Q., Qu, X., Zhai, J., Zhang, R.: Feasibility analysis of floating offshore wind turbine with single point mooring system. In: ISOPE International Ocean and Polar Engineering Conference, p. (2017). ISOPE
47. Armesto, J.A., Guanche, R., Jesus, F.D., Iturrioz, A., Losada, I.J.: Comparative analysis of the methods to compute the radiation term in cummins' equation. J. Ocean Eng. Mar. Energy **1**(4), 377–393 (2015)
48. OSC: OSC Services. https://osc.no/
49. Algoryx dynamics: Algoryx Dynamics Documentation. https://www.algoryx.se/documentation/complete/agx/655tags/latest/doc/UserManual/source/index.html
50. Nihei, Y., Iijima, K., Murai, M., Ikoma, T.: A comparative study of motion performance of four different FOWT designs in combined wind and wave loads. In: International Conference on Offshore Mechanics and Arctic Engineering, vol. 45493, pp. 007–05025 (2014). American Society of Mechanical Engineers
51. Wang, L., Jonkman, J., Papadopoulos, J., Myers, A.T.: Openfast modeling of the T-Omega Wind floating offshore wind turbine system. In: International Conference on Offshore Mechanics and Arctic Engineering, vol. 87578, pp. 001–01017 (2023). American Society of Mechanical Engineers
52. Brito, M., Ferreira, R.M., Teixeira, L., Neves, M.G., Canelas, R.B.: Experimental investigation on the power capture of an oscillating wave surge converter in unidirectional waves. Renew. Energy **151**, 975–992 (2020)
53. Bretschneider, C.L.: Generation of waves by wind: State of the art. Lecture notes prepared for a NATO short course in cooperation with Nuffic; Lunteren, September 1964. (1964)
54. Hansen, C.L., Bredmose, H., Vincent, M., Steffensen, S.E., Pegalajar-Jurado, A., Jensen, B., Dixen, M.: Resonant response of a flexible semi-submersible floating structure: experimental analysis and second-order modelling. J. Fluid Mech. **982**, 7 (2024)
55. Nagumo, T., Suzuki, H., Houtani, H., Takaoka, M., Gonçalves, R.T.: Experimental and numerical studies on regular wave responses of a very-light FOWT with a guy-wired-supported tower: Effects of wave height, wave direction, and mooring line configuration. Ocean Eng. **295**, 116844 (2024)